
Since January 2020 Elsevier has created a COVID-19 resource centre with free information in English and Mandarin on the novel coronavirus COVID-19. The COVID-19 resource centre is hosted on Elsevier Connect, the company's public news and information website.

Methods 90 (2015) 57–64

Contents lists available at ScienceDirect

Methods

journal homepage: www.elsevier.com/locate/ymeth

Review Article

# Methods for the characterization of stress granules in virus infected cells

Marc D. Panas [a], Nancy Kedersha [b], Gerald M. McInerney [a,*]

[a] Department of Microbiology, Tumor and Cell Biology, Karolinska Institutet, Stockholm, Sweden
[b] Division of Rheumatology, Immunology and Allergy, Brigham and Women's Hospital, Boston, MA, USA

ARTICLE INFO

*Article history:*
Received 26 February 2015
Received in revised form 8 April 2015
Accepted 9 April 2015
Available online 18 April 2015

*Keywords:*
Translation
Virus
Stress granules
Signaling
Cell biology

ABSTRACT

Stress granules are induced in many different viral infections, and in turn are inhibited by the expression of viral proteins or RNAs. It is therefore evident that these bodies are not compatible with efficient viral replication, but the mechanism by which they act to restrict viral gene expression or genome replication is not yet understood. This article discusses a number of methods that can be employed to gain a more complete understanding of the relationship between cellular SGs and viral RNA and protein synthesis in cells infected with diverse viruses.



## 1. Introduction

### 1.1. Stress granules

Stress granules (SG) are dynamic assemblies of ribonucleoprotein particles (mRNPs), which are formed in the cytoplasm of cells under many types of environmental stress [1,2]. The sequestration of mRNAs into these translationally-stalled cytoplasmic foci results from the rapid redirection of translation from housekeeping proteins to heat-shock proteins and other stress response factors. Upon detection of stress conditions, housekeeping mRNAs are triaged into SGs to conserve metabolic energy and to allow newly transcribed mRNAs for stress response factors to be efficiently translated.

Translation initiation under normal conditions requires the concerted activity of many cellular proteins known as eukaryotic initiation factors (eIFs). In brief, translation is enhanced when capped mRNAs are circularized by the cap-binding complex (eIF4F) and PABP, promoting their recruitment to the eIF3/40S ribosomal subunit complex. Subsequent recruitment of the 60S subunit and translation initiation at an AUG codon requires the ternary complex of eIF2, GTP and the methionyl initiator tRNA (eIF2–GTP–$tRNA_i$Met). SGs are formed when translation is blocked at the initiation stage by a number of different conditions [3], for example, inhibition of eIF4F activity or by eIF2α phosphorylation, which reduces the levels of eIF2–GTP–$tRNA_i$Met. When initiation is stalled, RNA binding proteins such as TIA-1 and TIAR can bind to the abortive complexes and relocalize them to form SGs [3]. When initiation factors become available again, for example when stress is relieved, SGs are disassembled as translation resumes. Assembly of the granules is also dependent on the Ras-GAP SH3 domain binding proteins 1 and 2 (collectively referred to as G3BP) [4]. G3BP proteins contain a nuclear transport factor-2 (NTF2)-like domain and the N-terminus and RNA binding domains closer to the C-terminus, both of which are necessary for SG formation [4]. The NTF2-like domain binds a number of partners, such as USP10 and CAPRIN-1, and also mediates dimerization. The ability of G3BP to nucleate SGs is regulated by phosphorylation of serine 149 [4]. CAPRIN-1 is necessary for normal progression through the G1-S cell cycle restriction point [5] and ubiquitin specific protease 10 (USP10) promotes the stability of a number of important proteins, including p53 [6]. Complexes containing G3BP and its many binding partners are thus involved in numerous cellular processes and likely involved in many signaling pathways [7].

In this review, we will discuss some methods for characterization of SGs in virus-infected cells. We discuss microscopy-based methods for revealing the localization of cellular and viral proteins and RNAs, as well as a newly-developed assay for SG protein solubility. We provide detailed protocols and reagent details for selected assays.

## 2. Importance of stress granules in viral infection

The first hint that SGs are important during viral infection came from the observation that the SG protein TIAR was bound and

* Corresponding author at: Department of Microbiology, Tumor and Cell Biology, Karolinska Institutet, Box 280, S-171 77 Stockholm, Sweden.
*E-mail address:* gerald.mcinerney@ki.se (G.M. McInerney).

http://dx.doi.org/10.1016/j.ymeth.2015.04.009
1046-2023/

sequestered by Sendai virus RNAs [8]. We subsequently showed that Semliki Forest virus (SFV) infection induces a transient wave of SGs early in infection that are triggered by eIF2α phosphorylation, but that SGs were not detected later in infection despite continued eIF2α phosphorylation [9]. The activation of the responsible eIF2α kinase, double stranded RNA activated protein kinase (PKR), is caused by viral dsRNA replication intermediates present in the cytoplasm in the initial stages of infection. The resulting SGs are subsequently disassembled by a virus-specific mechanism as viral RNA replication progresses [9]. Since those initial reports, studies have shown that all the major families of RNA viruses as well as several DNA viruses inhibit the induction of the SG response very soon after infection (reviewed in [10]). A common theme is their transient induction at early times in infection, followed by virus-directed block in formation of SGs to relieve the restriction on viral gene expression. Poliovirus disrupts SG assembly by mediating cleavage and degradation of G3BP1 [11], while other picornaviruses block SGs by different mechanisms [12]. Our recent work showed that the alphaviruses, including SFV and Chikungunya virus, disassemble SGs via the binding and sequestration of the SG proteins G3BP1 and G3BP2 mediated by the viral non-structural protein 3 (nsP3) [13–15]. Importantly, we showed that a viral mutant (SFV-F3A) unable to bind and sequester G3BP1/2 was attenuated for growth in vitro, but grew to titers equal to those of WT SFV in cells unable to form phospho-eIF2α-dependent SGs. This confirms that the main function of G3BP sequestration is to inhibit SGs, and that without this, SFV replicates poorly in WT cells. Clearly, SGs are an important facet of the early cell-intrinsic resistance against infection, but many details about their activity remain to be revealed. Such knowledge would help to identify targets for therapeutic intervention.

### 2.1. Special considerations for studying SGs in virus infected cells

The special and diverse environments in virus-infected cells present some particular considerations for the study of SGs. Virus replication alters the cellular environment in ways that promote viral genome replication, transcription, particle assembly and immune evasion. Often, cellular proteins are sequestered by viral factors and reassigned to functions that support rather than inhibit virus replication. SG proteins are no exception to this, with several examples of these proteins being co-opted by viruses to their own ends [13,15–18]. With this in mind, investigators need to concurrently use more than one marker to distinguish SGs from other foci, such as of accumulation of viral proteins with their cellular binding partners. It is advisable to double- or triple-stain with an SG marker such as TIA-1/R OR G3BP-1/2 in addition to an initiation complex protein such as eIF3, eIF4G or PABP. The dissolution of SGs by cycloheximide or emetine treatment can also be used to distinguish bona fide SGs from other foci of protein accumulation [19].

A common strategy for demonstrating viral inhibition of SG assembly has been to challenge virus-infected cells with an exogenous stress inducer, such as sodium arsenite (SA) to determine if virus-encoded factors act to block the induction of SGs by the exogenous inducer. SA activates the heme-regulated inhibitor (HRI) kinase, which phosphorylates eIF2α, in turn inducing SGs [20,21]. However, this approach is complicated by the activation of another eIF2α kinase (PKR), triggered by diverse virus infections. In cells infected with viruses that induce phosphorylation of eIF2α, the addition of arsenite is redundant and does not lead to formation of SGs in infected cells, even if there is no virus-encoded mechanism to block their formation. For example, in SFV-infected cells, PKR becomes activated early in infection by the presence of dsRNA replication intermediates. Despite the consequent high and sustained levels of phosphorylated eIF2α, translation of the viral sub-genomic mRNA is efficient due to the presence of a translational enhancer in the capsid coding region [9]. To avoid this complication, researchers should consider using a phospho-eIF2α-independent SG inducer (see Table 1), such as pateamine A (Pat A, [22]) or hippuristanol [23], which inhibit the RNA helicase eIF4A, a component of the eIF4F complex, leading to SG formation independently of eIF2α Cells infected with WT SFV do not form SGs in response to either SA or Pat A, but a mutant which does not inhibit SG formation does form SGs in response to 50 nM Pat A, but not to SA [15].

## 3. Immunostaining – classical method for identification of SGs

SGs contents are in rapid flux in and out of the structures [19], confounding attempts to biochemically isolate them. The

**Table 1**
Commonly used SG inducing treatments.

| Treatment/reagent | Stock solution, if applicable | Conditions | Effects | Comments |
|---|---|---|---|---|
| Sodium arsenite Sigma S7400 | 65 mg/ml makes 0.5 M stock in PBS | 0.5-1.0 mM for 30–60 min | Induces SGs, phospho-eIF2α dependent | Commonly used SG inducer, works in all cells except eIF2α S51A mutants |
| Thapsigargin Sigma T9033 | 0.65 mg/ml makes 1.0 mM stock in DMSO | 1.0 μM for 30–90 min | Induces SGs, phospho-eIF2α dependent | Does not work on HeLa, DU145, and COS7 cells |
| Pateamine A Jerry Pelletier (McGill University) | DMDA-PatA 2.0 mM stock in DMSO | 50 nM for 30–60 min | Induces SGs, phospho-eIF2α independent | Blocks eIF4A helicase activity |
| Hippuristanol Jerry Pelletier (McGill University) | Stock 10 mM in DMSO | 1 μM for 30–60 min | Induces SGs, phospho-eIF2α independent | Blocks eIF4A helicase activity |
| 2-Deoxy-D-glucoseSigma D8375 | 164 mg/ml makes 1 M stock in $H_2O$ | 250 mM in HBSS or PBS 60–90 min | Induces SGs, phospho-eIF2α independent | Can be combined with FCCP for total energy starvation |
| Oligomycin Sigma 75351 | 7.9 mg/ml makes 10 mM stock in DMSO | 10 μM for 60 min | Induces SGs, phospho-eIF2α independent | Blocks F1Fo ATPase |
| FCCP Sigma C2920 | 20 mg/ml makes 78 mM stock in DMSO | 78 μM for 1–2 h in glucose-free media | Induces SGs, phospho-eIF2α independent | Mitochondrial protein gradient abolished |
| Heat shock | Preheated incubator | 42–44°, 30–45 min | Induces SGs, phospho-eIF2α independent | Cells adapt and SGs can disappear within 1 h |
| Puromycin Sigma P9620 | 10 mg/ml makes 18.4 mM in $H_2O$ | 20 μg/ml for several hours | Induces large SGs | Disassembles ribosome, only ~20% cells respond; effects vary with cell line |
| Emetine Sigma E2375 | 100 mg/ml makes180 mM stock in $H_2O$ | 180 μM for 1–2 h | Disassembles SGs; blocks elongation and stabilized polysomes | Useful SG diagnostic |
| Cycloheximide Sigma C7698 | 50 mg/ml makes 177 mM stock in DMEM | 17–68 μM for 1–2 h | Disassembles SGs; blocks elongation and stabilized polysomes | Useful SG diagnostic |

structures are however readily visible in immunofluorescence microscopy using antibodies for SG marker proteins or in situ hybridization using oligo-dT probes to detect polyadenylated mRNAs. SGs can even be seen as phase dense structures in light microscopy [3]. We present a list of SG markers and specific antibodies for their detection in Table 2.

TIA-1/R and G3BP-1/2 are the most commonly used SG markers. Both are necessary for SG formation although the details of their individual roles remain elusive [4,19]. Both proteins contain RNA-binding sequences which are necessary for the assembly and integrity of SGs. Aggregation of prion-like domains at the C-termini of TIA-1/R is necessary for SG formation [24]. Other RNA-binding proteins that can both bind RNA and oligomerize are also localized to SGs. Examples are Fragile X Mental Retardation Protein (FMRP/FXR1) [23], p54/RCK [25], Staufen-1/2 [26] and tristetraprolin (TTP) [27]. As SGs differ in composition depending on the stress used to trigger their formation, universal SG markers should be used to confirm that an RNA granule is really a SG. Components of the canonical translation initiation complexes such as eIF4E, eIF4G, eIF3, PABP-1 and small but not large ribosomal subunits are used to identify all types of SGs [28]. The presence of initiation factors in the cytoplasmic foci implicates those foci as aggregates of stalled or abortive translation complexes. The presence of signaling proteins in virus-induced SGs has gained considerable attention recently [7]. The dsRNA-activated protein kinase (PKR) has been detected in SGs as a G3BP binding partner [29], while its main substrate eIF2α is found only in SGs induced by the inactivation of eIF4A. The cytoplasmic RNA receptors retinoic acid inducible gene I (RIG-I) [30] and melanoma differentiation-associated protein 5 (MDA5) [31] have been detected in SGs induced by mutants of influenza and cardiovirus, respectively, but it is less clear if their localization to SGs is required for signaling to the type I interferon pathway during infection with WT viruses.

Some factors appear to be specific for SGs induced by some conditions but not others. Sam68, a putative regulator of mRNA stability [32] was shown to be present in poliovirus-induced SGs [33] and in TIA-1-positive structures late in herpes simplex virus (HSV)-2 infection [34] but is not detected in those induced by Theiler's encephalomyelitis virus (TMEV) [12] or SFV (our unpublished observations). The polypyrimidine tract binding protein (PTB) was detected in TMEV induced SGs [12] and in TIA-1/R-positive foci in transmissible gastroenteritis coronavirus (TGEV)-infected cells but not in SA-induced SGs [35]. Poly-C binding protein 2 (PCBP2), which is involved in cap-independent translation, has been detected in heat and SA-induced SGs, likely via interaction with TIA-1 [36]. Another translation regulating protein, the cytoplasmic polyadenylation element-binding protein (CPEB) was found to localize to SGs, possibly via interaction with rck/p54 [25].

As a more complete picture emerges, the diversity of the composition of different virus-induced SGs is likely to reflect the diversity in mechanisms by which viruses modulate the translation apparatus in their host cells.

**Table 2**
Commonly used antibodies for SG components.

| Target | Company/cat number | Species | Optimal dilution (where known) | Comments |
|---|---|---|---|---|
| BrUTP | Enzo, ADI-MSA-200-E | Mouse | 100 | For labeling of nascent RNA |
| CAPRIN-1 | Sigma, HPA018126 | Rabbit | | SG marker, G3BP-binding partner |
| CAPRIN-1 | Proteintech Group 15112-1-AP | Rabbit | 1000 | SG marker, G3BP-binding partner |
| dsRNA | SCICONS English & Scientific Consulting, J2-1406 | Mouse | 200 | For labeling RNA replication complexes |
| eIF2α phospho | Abcam 32157 | Rabbit | 1000 | |
| eIF2α total | Cell Signaling 2103S | Mouse | | Present in Pat A SGs, not arsenite SGs |
| eIF3b | Santa Cruz, sc-16377 | Goat | 500 | SG marker |
| eIF4AI | Santa Cruz, sc-14211 | Goat | 200 | Target of pateamine A. SG marker |
| eIF4E | Santa Cruz, sc-13963 | Rabbit | 200 | May not detect mouse protein. eIF4E may also be found in PBs |
| eIF4E | Santa Cruz, sc-9976 | Mouse | 200 | eIF4E may also be found in PBs |
| eIF4G | Santa Cruz, sc-11373 | Rabbit | 200 | May not detect mouse protein |
| FMR1 | Santa Cruz, sc-101048 | Mouse | 200 | SG marker |
| FXR1 | Santa Cruz, sc goat 10554 | Goat | 200 | SG marker |
| G3BP-1 | Aviva (BioSite), ARP37713 | Rabbit | 200 | SG marker |
| G3BP-1 | Santa Cruz sc-81940 | Mouse | 200 | SG marker |
| G3BP-1 | BD, 611126 | Mouse | 200 | SG marker |
| G3BP-2 | Bethyl A302-040A | Rabbit | 1000 | SG marker |
| G3BP-2 | Bethyl A302-034A | Rabbit | 1000 | SG marker |
| G3BP-2 | Assay Biotech, c18193 | Rabbit | 500 | SG marker |
| HuR | Santa Cruz, sc-5261 | Mouse | 200 | SG marker |
| PABP-1 | Santa Cruz, sc-32318 | Mouse | 200 | SG marker |
| PKR | BD Biosciences 3224650 | Mouse | 200 | |
| PTB | InvitroGen 32-4800 | Mouse | | Cardiovirus |
| Puromycin | Millipore MABE343 | Mouse | 1000 | For labeling of nascent protein |
| RIGI | Cell Sig. 3743S; Cell Sig. 4200S | Rabbit | | |
| Sam68 | Santa Cruz SC -333 | Rabbit | | Present in UV-induced SGs |
| Staufen | Proteintech Group, 14225-1-AP | Rabbit | 500 | SG marker |
| TIA-1 | Santa Cruz, sc-1751 | Goat | 200 | SG marker |
| TIAR | Santa Cruz, sc-1749 | Goat | 200 | SG marker |
| USP10 | Abcam, ab72486 | Rabbit | 400 | SG marker, G3BP-binding partner |
| USP10 | PTG 19374-1-AP | Rabbit | 200 | SG marker, G3BP-binding partner |
| USP10 | Bethyl A300-900A1 | Rabbit | 400 | Human, not mouse; SG marker, G3BP-binding partner |
| USP10 | Bethyl A300-901A1 | Rabbit | 400 | Human, not mouse; SG marker, G3BP-binding partner |
| YB-1 | Proteintech Group 20339-1-AP | Rabbit | 1000 | SG (and PB) marker |

This table presents a list of SG components and other targets of investigation described in this review. For each, we present an optimal dilution, which worked best in our hands. Readers should experimentally verify the optimal dilution for each lot of antibody, fixation protocols and other conditions.

### 3.1. Regular double/triple staining

The aggregation of TIA-1/R [34,37] and G3BP1/2 [15,38] has been detected in non-SG structures in virus infections, so double or triple staining for SG component molecules must always be performed in order to confirm the existence of canonical SG in virus infection. Enforced disassembly of SGs using inhibitors of elongation (emetine, cycloheximide) is easy to do and strongly recommended.

Protocol:

1. Grow cells on coverslips in 12- or 24-well plates and perform infection experiment so that cells are at approximately 70–90% confluency at time of fixation. Include a positive control of cells treated with known SG inducers (Table 1).
2. Rinse cells 1–3 times with 1 mL of PBS at RT.
3. Remove PBS and immediately fix (do not allow cells to dry out) in 4% paraformaldehyde (PFA) in PBS for 10–15 min with rocking.
4. Remove PFA and immediately permeabilise in 100% methanol at −20 °C for 10 min. Users may wish to test 0.5% Triton in PBS as an alternative permeabilization method for some antibodies.
5. *Optional:* Incubate cells in 70% ethanol for up to one week storage at + 4 °C or indefinitely at −20 °C.
6. Wash cells 1–3 times with 1 mL PBS at RT, 5 min each wash with rocking
7. Incubate in blocking buffer for 60 min at room temperature with rocking. Blocking solution: 5% normal horse serum (Sigma H1270), made up in PBS containing 0.02% sodium azide. Horse serum is used when secondary antibodies are from donkey. If using another species of secondary antibody, blocking should be done using the serum of that species.
8. Prepare primary antibody mix using the best experimentally determined dilutions (Table 2) in blocking solution, and incubate the cells in primary antibody for 45 min to 2 h at RT with rocking.
9. *Optional:* Incubate primary antibody mix overnight at 4 °C.
10. Wash cells three times in PBS, 5 min each wash, with rocking.
11. Incubate secondary antibody mix using the best experimentally determined dilution in blocking buffer for 1–2 h at RT. We typically triple-stain using ML (“multiple labeling”) grade fluorescent conjugated antibodies from Jackson Immunoresearch. Cy2 and Cy5 conjugates are diluted 1:200, whereas Cy3 conjugates are diluted 1:2000. We routinely add 0.05 μg/ml Hoechst 33258 dye to the secondary antibody cocktail in order to visualize cell nuclei.
12. Wash cells 3 times in PBS, 5 min each wash, with rocking.
13. Mount coverslips using a polyvinyl-based mounting medium. Store in the dark. The slides are usually stable for several weeks.

Colocalization can be quantified using a number of in silico analyses (reviewed in [39]). However, since only a subset of the total cellular pool of SG proteins is found in SGs at any particular time, the colocalization coefficients may be quite low, even following SA or Pat A treatment. An alternative, more sensitive method for confirming functional colocalization of two proteins is the proximity ligation assay (available in a kit from Sigma, “Duolink using PLA technology”), which has been used to demonstrate the localization of PKR and G3BP in poliovirus induced SGs [29].

### 3.2. Puromycin labeling

Viruses are dependent on host cell ribosomes for the synthesis of viral proteins. Thus, the appropriation of cellular ribosomes for the translation of viral mRNAs is a critical point in the early interactions between viruses and their host cells. In many of the infected cells that have been analyzed, SGs appear at times that coincide with the change in protein production profile from exclusively cellular to mainly viral. It may be useful to know the levels of total translation in cells undergoing this change and to relate those levels to the appearance of SGs.

A ribopuromycylation staining method can be used to visually quantify the levels of translation in cells using conventional fluorescence microscopy. Puromycin is a broadly-acting antibiotic which blocks translation by entering the A site of both prokaryotic and eukaryotic ribosomes, and is itself transferred to the growing polypeptide chain, causing the disassembly of polysomes and release of the truncated polypeptide containing puromycin instead of a normal amino acid at its C-terminus. Treatment of cells for very short times with 10 μg/ml puromycin leads to cessation of translation and the release of the puromycinylated nascent chains from polysomes. David and colleagues showed that a puromycin-specific antibody could be used with immunofluorescence microscopy to detect puromycinylated proteins and thus to determine the relative levels and distribution of translation in cells [40]. While other in vivo protein labeling techniques (notably, incorporation of azido-modified amino acid analogs, e.g. Invitrogen “click-it” chemicals) can be used to label and detect protein translation in situ, they require prestarving the cells in methionine-free media, which may perturb normal infection kinetics and other aspects of metabolism. Puromycin labeling has several advantages: it is compatible with a broad range of drugs (including SA and Pat A), it is very quick, and compatible with immunostaining for other SG markers.

Protocol:

1. Grow cells on coverslips and perform infection experiment so that cells are at approximately 50–90% confluency at time of fixation.
2. Incubate cells in complete medium containing 10 μg/ml puromycin for 5 min at 37 °C. Note that David et al. recommend adding 208 μM emetine in order to limit the extent of puro incorporation to 1 molecule of puro per mRNA [41]. Use cells without puromycin incubation as a negative control.
3. Rinse the cells 1–3 times with 1 ml of PBS
4. Fix for 10–15 min in 4% PFA in PBS
5. Permeabilise in MeOH or Triton as appropriate (see Section 3.1) and process for immunofluorescence using puromycin-specific antibody (Millipore MABE343 mouse monoclonal at 1/1000 dilution), counterstaining with other antibodies as appropriate.

We have used this technique to determine the relationship between transient SGs, the newly assembled viral RNA replication complexes and the rate and location of protein synthesis in SFV-infected cells at different times post-infection. Mouse embryonic fibroblasts (MEFs) were infected with wt SFV at a multiplicity of infection (MOI) of 0.5. At various times post infection, 10 μg/mL puromycin was added to the media for 5 min immediately prior to fixation and staining for nsP3, TIA-1 and puromycin. Representative images are presented in Fig. 1. In mock-infected cells, TIA-1 is predominantly located in the nucleus, while the puromycin signal is strong and not located in any specific cytoplasmic compartment. As we have described before, at approximately 2–4 hpi, TIA-1 translocates to the cytoplasm and is transiently detected in SGs. However, in region of the cytoplasm where viral protein or RNA is detected, SGs are no longer visible [9]. At this point, the total translation rate in the infected cell is drastically reduced as compared to mock-infected cells. Later, as the SGs are entirely disassembled and viral RCs are distributed throughout the cytoplasm, translation rate is increased again. This data agrees

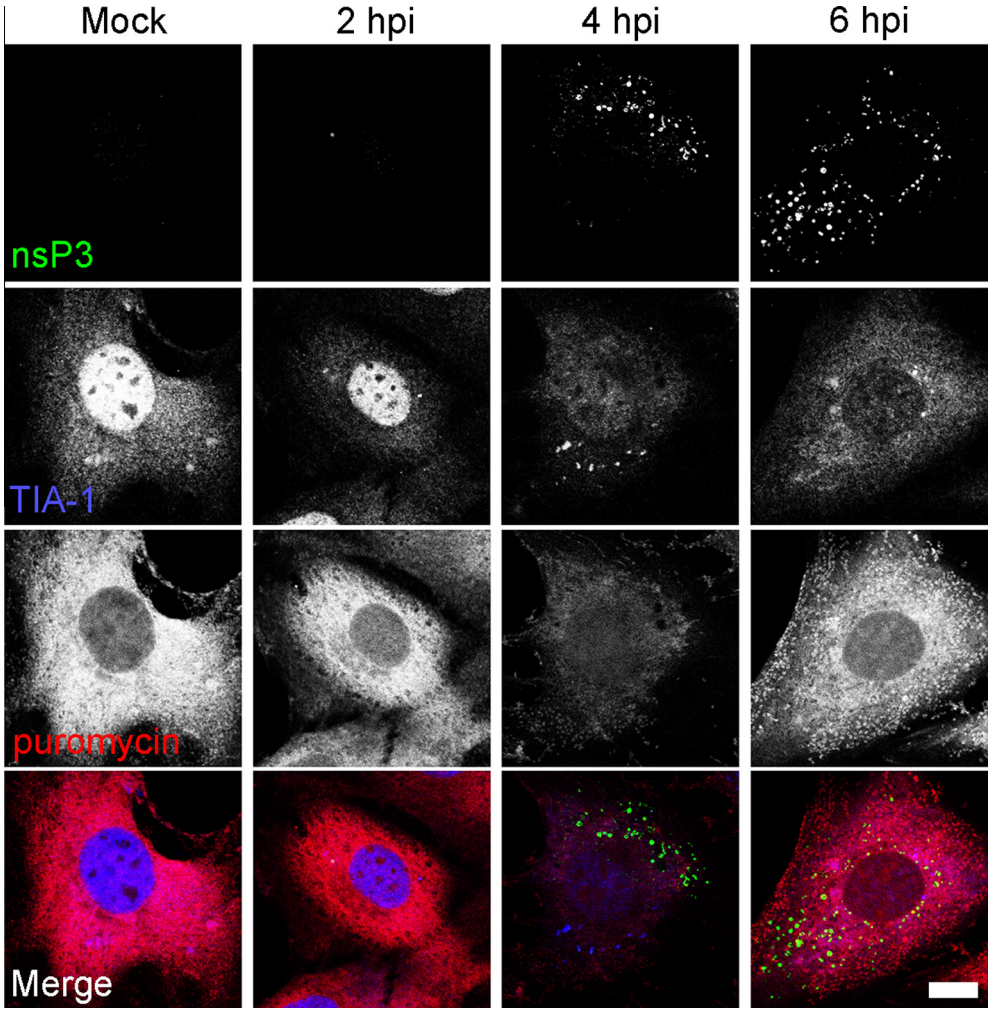


**Fig. 1.** Ribopuromycylation method reveals that the transient SG assembly in SFV-infected cells coincides with inhibition of cellular translation. MEFs grown on coverslips were infected with wt SFV at MOI 0.5. Cells were fixed at the indicated times post infection after a 5 min treatment with 10 μg/ml puromycin, and stained for SFV nsP3 (green), TIA-1 (blue) and puromycin (red). Images were processed using Adobe Photoshop. Bar = 20 μm.

with $^{35}$S methionine labeling data [9], and demonstrates the strong correlation between the assembly/disassembly of SGs with the shut-off of host cell translation, thus illustrating the power of this technique for the study of localized translation (or its absence) in virus-infected cells.

### 3.3. In vivo labeling of nascent viral RNA with BrUTP

Since the function of SGs appears linked to the triage of mRNA, it is reasonable to assume that SGs induced during viral infection might sequester viral mRNAs in order to inhibit their translation. To examine the relationship between viral RNA replication complexes and SGs, it is useful to visualize nascent viral RNA in situ and co-stain for SG marker(s). A number of techniques are available for co-staining RNA and protein, such as fluorescence in situ hybridization (FISH) and 5-bromourudine 5′-triphosphate (BrUTP) labeling. An antibody specific for dsRNA (SCICONS English & Scientific Consulting, J2-1406) can also be used to label sites of viral RNA synthesis in cells infected with many types of virus [42]. Similar to puromycin labeling, BrUTP labeling involves incubating cells with modified ribonucleotide BrUTP to allow its incorporation into nascent RNA, followed by the immunodetection of BrUTP using a specific antibody (Enzo) [43]. BrUTP uptake into cells is facilitated by transfection. This technique allows the detection of viral RNAs, which may be localized to SGs during infection. Its major advantage over in conventional in situ hybridization and dsRNA staining, if used together with actinomycin D (Act D; see below) to block host cellular transcription, it is selective for newly synthesized viral RNA produced during short times during infection. In our previous work [9], we used in vivo BrUTP labeling to identify nascent SFV RNA in combination with TIA-1 immunostaining to identify SGs. We found that, when present in virus-infected cells, the SGs were typically located in regions of the cell devoid of newly produced viral RNA. As the infection progressed, and viral replication complexes were distributed throughout the cytoplasm, SGs were no longer detectable. We did not detect BrUTP labeled viral RNA in SGs, in agreement with FISH results that did not detect viral RNA in SGs.

Alphavirus infection profoundly inhibits the synthesis of cellular RNA [44]. Short times after infection, pulse-labeled RNA will consist almost entirely of viral RNA [44,45]. However, for other RNA viruses, BrUTP staining may label both viral and cellular RNA, confounding interpretation of staining. Since viral RNA-dependent RNA polymerases are not sensitive to actinomycin D (Act D), this inhibitor can be used during BrUTP labeling to ensure that only viral RNAs incorporate the BrUTP. Act D inhibits DNA-dependent transcription by binding DNA template and preventing mRNA elongation by RNA polymerases, but does not bind RNA. Fig. 2A shows MEFs after staining with BrUTP for 1 h in the presence or absence of Act D. In non Act D-treated cells, BrUTP staining is brightest in the nucleoli, the sites of ribosomal RNA synthesis.

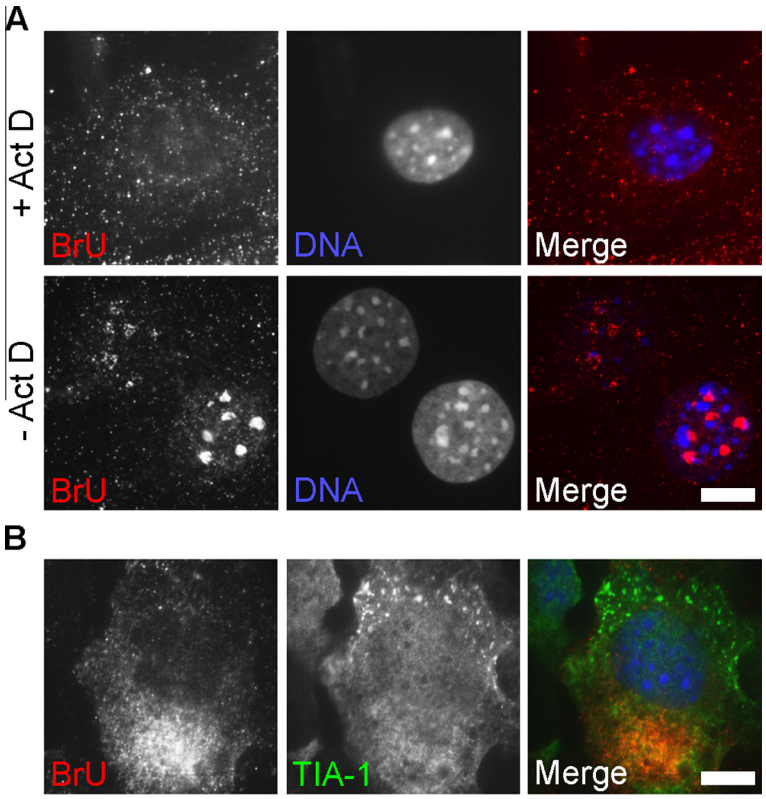


**Fig. 2.** The transient appearance of SGs in SFV-infected cells negatively correlates with the assembly of RNA replication complexes. (A) MEFs grown on coverslips were mock-treated or treated with 1 μg/mL Act D for 30 min prior to and including 1 h of BrUTP labeling. Cells were fixed and stained for BrU (red) and DNA (blue). Images were processed using Adobe Photoshop. Bar = 20 μm. (B) MEFs grown on coverslips were infected with wt SFV at MOI 0.5. At 4 hpi, BrUTP was added according to protocol. Cells were fixed at 5hpi and stained for TIA-1 (green) and BrU (red). Images were processed using Adobe Photoshop. Bar = 20 μm.

Different intensities of BrUTP staining reflect different efficiencies of transfection of the nucleotide in individual cells.

Protocol:

1. Grow cells on coverslips in 12-well plates and perform infection experiment so that cells are at approximately 70–90% confluency at time of fixation.
2. *Optional:* 30 min before each labeling period, medium is replaced with complete medium containing 1 μg/mL Act D. Note that Act D is often difficult to solubilize; Actinomycin D-mannitol from Sigma (A5156) is formulated to avoid this problem and is water soluble.
3. Medium is removed and replaced with 450 μL OptiMEM (Invitrogen).
4. Prepare a mixture containing 45 μL OptiMEM, 10 mM BrUTP (Sigma B7166) and 5 μL Lipofectamine 2000 reagent (Invitrogen). Incubate at RT for 15 min and pipette slowly onto cells.
5. Incubate cells for desired labeling time at 37 °C.
6. Wash cells 3 times in ice-cold PBS.
7. Fix for 15 min in 4% PFA in PBS at room temp with shaking.
8. Permeabilize in MeOH/Triton as appropriate (see Section 3.1).
9. Stain with BrUTP-specific antibody (Table 1).

We infected MEFs with wt SFV at MOI 0.5, and labeled total RNA using a 1-h incubation with BrUTP in the presence of Act D (between 4 and 5 hpi; Fig. 2B). Under these conditions, no RNA staining was detected in nucleoli. In cells where SGs were visible, nascent viral RNA staining was always located contralateral to the TIA-1-positive SGs. A representative image is shown in Fig. 2B.

## 4. Analysis of SG components using biotin-isoxazole fractionation

Although the biochemical isolation of SGs has proven impossible to date, a technique was recently developed which allows the cell-free formation of SG-associated proteins and RNA precipitates. Isoxazole is a small molecule known to induce the differentiation of stem cells [46], and a biotinylated version (B-isox) was recently shown to precipitate a subset of RNA-binding proteins and RNAs in a temperature-dependent manner from cell lysates [47,48]. These precipitated proteins were highly enriched in SG-associated proteins and protein components of other types of RNA granules [48]. Most B-isox precipitating proteins contain low-complexity (LC), unstructured regions of unknown function, and these LC regions are necessary and sufficient for their precipitation by B-isox. These studies led the McKnight laboratory [48] to propose that RNA granule assembly is mediated by a concentration and temperature dependent liquid/liquid phase transition. Although the mechanism of B-isox precipitation is not well understood, using B-isox precipitation to selectively precipitate SG-competent proteins can serve as a surrogate method for crude purification of SG components, essentially mimicking stress in vitro. The assay involves the simple addition of the B-isox to cell lysates, incubation with agitation at 4 °C, followed by centrifugation to separate the precipitate and supernatant fractions and analysis by SDS–PAGE.

Reagents:

*B-isox:*6-(5-(Thiophen-2-yl) isoxazole-3-carboxamido)hexyl 5-((3a*S*,4*S*,6a*R*)-2-oxohexahydro-1*H*-thieno[3,4-*d*]imidazol-4-yl)pentanoate, (Sigma catalog number T51161-1MG). Vial contains 1 mg;

dilute contents in 192 μL DMSO to obtain a 10 mM (100×) stock solution. Store at −20 °C.

Protocol:

1. Lyse cells in EE buffer (50 mM HEPES pH 7.5, 150 mM NaCl, 0.1% NP40, 1 mM EDTA, 2.5 mM EGTA, 10% glycerol, 1 μM DTT or 20 mM β-mercaptoethanol) supplemented with protease, phosphatase, and RNase inhibitors (optional). Extract with tumbling at 4 °C for 20 min, then centrifuge for 15 min at maximum speed in a refrigerated eppendorf microcentrifuge. Remove supernatant and save a small fraction of for SDS–PAGE analysis as "input".
2. Divide the remaining cleared lysate in half. Add 1/100 dilution of 10 mM b-isox in DMSO to final concentration of 100 μM. Add 1/100 dilution of DMSO to the mock control. *Optional:* add RNase A at 20 μg/mL and tumble lysate in cold for 1 h prior to addition of B-isox.
3. Tumble in cold room 90 min
4. Spin 10,000*g* for 10 min at 4 °C.
5. Harvest the supernatant from both B-isox and mock-treated samples, and add equal volume of 2× reducing SDS–PAGE loading buffer. These samples will be used to compare the percent of individual proteins removed by B-isox precipitation.
6. Wash pellet twice by suspending in ice-cold EE buffer, vortexing, and incubation for 10 min on ice, followed by centrifugation at 10,000*g* for 10 min at 4 °C.
7. Resuspend B-isox and mock pellets in reducing SDS–PAGE loading buffer and analyze supernatant and pellet fractions by SDS–PAGE and immunoblotting.
8. Quantification of the band intensities can be performed using Image J.
9. *Optional:* Stain gel to see bands. Note that silver stain will detect both proteins and nucleic acid, whereas Coomassie or Ponceau will detect only proteins.

We used this technique to determine the B-isox solubility of G3BP1 and its binding partners in cells expressing EGFP-fusion proteins carrying the G3BP-binding motifs from SFV nsP3, described in [15]. U2OS cell lines stably expressing low and high levels of EGFP-31-wt (clones 1 and 8, respectively) or a non-G3BP-binding version (EGFP-31-F3A) were lysed and subjected to B-isox precipitation in the presence or absence of RNase and analyzed using SDS–PAGE. Gels containing lysates, supernatants and B-isox precipitates were silver stained to confirm equal protein loading and to demonstrate that precipitation only occurred in the presence of B-isox (Fig. 3A and B). Replicate samples were resolved on SDS–PAGE and transferred to nitrocellulose for immunoblotting (Fig. 3C). The general profile of proteins precipitating with B-isox was similar to expected [48], and did not change appreciably with expression of either EGFP-31-wt or -F3A. RNase pretreatment of the lysates removed the high molecular mass bands (identified as RNA by their failure to stain with protein stains, data not shown), and resulted in the precipitation of a number of smaller bands identified as ribosomal proteins (data not shown). When pelleted material was analyzed by immunoblotting for SG proteins, we observed that CAPRIN-1, eIF3b and TIAR all precipitated equally well from cells expressing low or high levels of EGFP-31-wt or EGFP-31-F3A (Fig. 3C). However, G3BP-1 and -2

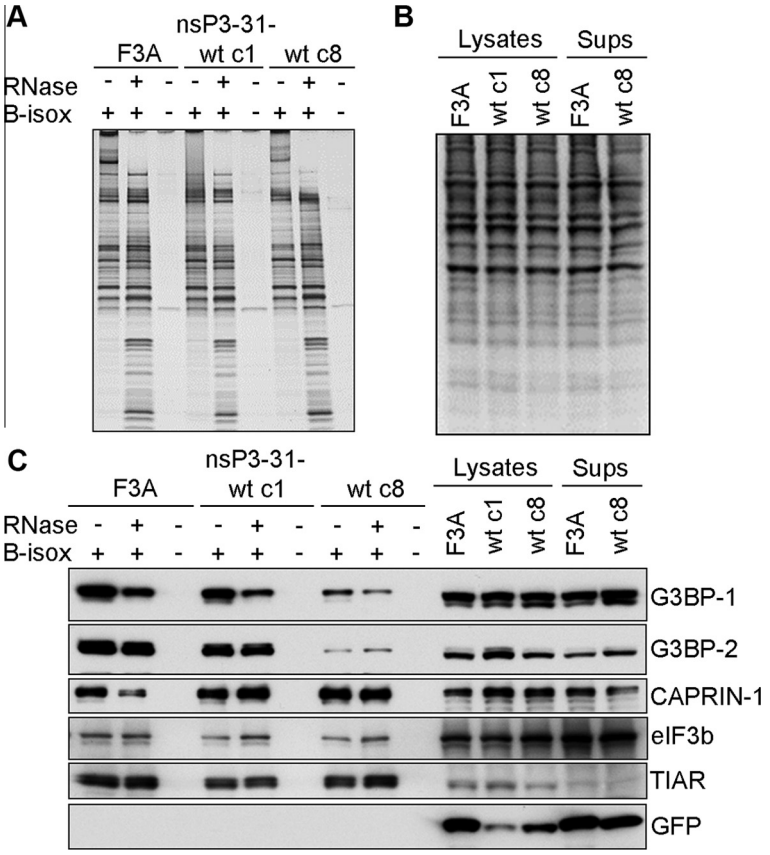


**Fig. 3.** Overexpression of FGDF-containing proteins alters the B-isox solubility of G3BP-1 and -2. Lysates from U2OS cells expressing low (clone 1, c1) or high (clone 8, c8) levels of EGFP-31-wt or high levels of EGFP-31-F3A were subjected to B-isox precipitation in the presence or absence of RNase. (A) B-isox pelleted material or (B) lysates and supernatants were analyzed by SDS–PAGE and silver staining. (C) B-isox pellets, supernatants and total lysates were analyzed by immunoblotting for G3BP-1, G3BP-2, CAPRIN-1, eIF3b, TIAR or GFP.

precipitation was inhibited in cells expressing high levels of EGFP-31-wt (clone 8), indicating that the EGFP-31-wt/G3BP interaction alters it such that it is no longer "SG competent" by this criterion. This result is in agreement with our previous work showing that overexpression of EGFP-31-wt but not EGFP-31-F3A blocks the formation of SA-induced SGs [14]. Further description of the use of B-isox to determine solubility of SG proteins will be published elsewhere.

## 5. Conclusions

The number of reports implicating SGs in various diverse viral life cycles is increasing [49] and now includes members of most families of RNA viruses and several DNA viruses. Mutant viruses, which fail to inhibit the SG response are attenuated in vitro [8,14,15,50], and it is therefore becoming more obvious that SGs represent a very early, cell-intrinsic antiviral defense mechanism. It is therefore not surprising that so many viruses encode proteins or RNAs that inhibit the formation of SGs on viral mRNAs. The condensation of mRNPs into SGs creates defined subcellular regions that recruit/divert a host of signaling molecules, suggesting that SGs constitute RNA-dependent signaling hubs that communicate a "state of emergency" [7] to the rest of the cell, and link SG formation to apoptosis. These signaling functions of SGs will likely prove critical to their anti-viral activity. However, despite recent progress, much remains to be learned about SG functions in viral replication. The techniques described here will facilitate further investigations into mechanisms of SG-mediated viral restriction and viral evasion strategies.

## Acknowledgements

We thank Benjamin Götte and Bastian Thaa for technical help. This work was supported by Grants from the Swedish Cancer Society and the Swedish Research Council to G.M.M.

## References

[1] P. Anderson, N. Kedersha, Curr. Biol. 19 (2009) R397–R398.
[2] J.R. Buchan, R. Parker, Mol. Cell 36 (2009) 932–941.
[3] N.L. Kedersha, M. Gupta, W. Li, I. Miller, P. Anderson, J. Cell Biol. 147 (1999) 1431–1442.
[4] H. Tourriere, K. Chebli, L. Zekri, B. Courselaud, J.M. Blanchard, E. Bertrand, J. Tazi, J. Cell Biol. 160 (2003) 823–831.
[5] S. Solomon, Y. Xu, B. Wang, M.D. David, P. Schubert, D. Kennedy, J.W. Schrader, Mol. Cell. Biol. 27 (2007) 2324–2342.
[6] J. Yuan, K. Luo, L. Zhang, J.C. Cheville, Z. Lou, Cell 140 (2010) 384–396.
[7] N. Kedersha, P. Ivanov, P. Anderson, Trends Biochem. Sci. 38 (2013) 494–506.
[8] F. Iseni, D. Garcin, M. Nishio, N. Kedersha, P. Anderson, D. Kolakofsky, EMBO J. 21 (2002) 5141–5150.
[9] G.M. McInerney, N.L. Kedersha, R.J. Kaufman, P. Anderson, P. Liljeström, Mol. Biol. Cell 16 (2005) 3753–3763.
[10] R.E. Lloyd, PLoS Pathog. 8 (2012) e1002741.
[11] J.P. White, A.M. Cardenas, W.E. Marissen, R.E. Lloyd, Cell Host Microbe 2 (2007) 295–305.
[12] F. Borghese, T. Michiels, J. Virol. 85 (2011) 9614–9622.
[13] M.D. Panas, T. Ahola, G.M. McInerney, J. Virol. 88 (2014) 5888–5893.
[14] M.D. Panas, T. Schulte, B. Thaa, T. Sandalova, N. Kedersha, A. Achour, G.M. McInerney, PLoS Pathog. 11 (2015) e1004659.
[15] M.D. Panas, M. Varjak, A. Lulla, K.E. Eng, A. Merits, G.B. Karlsson Hedestam, G.M. McInerney, Mol. Biol. Cell 23 (2012) 4701–4712.
[16] M.M. Emara, M.A. Brinton, Proc. Natl. Acad. Sci. U.S.A. 104 (2007) 9041–9046.
[17] G.C. Katsafanas, B. Moss, Cell Host Microbe 2 (2007) 221–228.
[18] W. Li, Y. Li, N. Kedersha, P. Anderson, M. Emara, K.M. Swiderek, G.T. Moreno, M.A. Brinton, J. Virol. 76 (2002) (2000) 11989–12000.
[19] N. Kedersha, M.R. Cho, W. Li, P.W. Yacono, S. Chen, N. Gilks, D.E. Golan, P. Anderson, J. Cell Biol. 151 (2000) 1257–1268.
[20] N.L. Kedersha, M. Gupta, W. Li, I. Miller, P. Anderson, J. Cell Biol. 147 (1999) 1431–1441.
[21] T. Ohn, N. Kedersha, T. Hickman, S. Tisdale, P. Anderson, Nat. Cell Biol. 10 (2008) 1224–1231.
[22] Y. Dang, N. Kedersha, W.K. Low, D. Romo, M. Gorospe, R. Kaufman, P. Anderson, J.O. Liu, J. Biol. Chem. 281 (2006) 32870–32878.
[23] R. Mazroui, R. Sukarieh, M.E. Bordeleau, R.J. Kaufman, P. Northcote, J. Tanaka, I. Gallouzi, J. Pelletier, Mol. Biol. Cell 17 (2006) 4212–4219.
[24] N. Gilks, N. Kedersha, M. Ayodele, L. Shen, G. Stoecklin, L.M. Dember, P. Anderson, Mol. Biol. Cell 15 (2004) 5383–5398.
[25] A. Wilczynska, C. Aigueperse, M. Kress, F. Dautry, D. Weil, J. Cell Sci. 118 (2005) 981–992.
[26] M.G. Thomas, L.J. Martinez Tosar, M. Loschi, J.M. Pasquini, J. Correale, S. Kindler, G.L. Boccaccio, Mol. Biol. Cell 16 (2005) 405–420.
[27] G. Stoecklin, T. Stubbs, N. Kedersha, S. Wax, W.F. Rigby, T.K. Blackwell, P. Anderson, EMBO J. 23 (2004) 1313–1324.
[28] N. Kedersha, S. Chen, N. Gilks, W. Li, I.J. Miller, J. Stahl, P. Anderson, Mol. Biol. Cell 13 (2002) 195–210.
[29] L.C. Reineke, R.E. Lloyd, J. Virol. 89 (2015) 2575–2589.
[30] K. Onomoto, M. Jogi, J.S. Yoo, R. Narita, S. Morimoto, A. Takemura, S. Sambhara, A. Kawaguchi, S. Osari, K. Nagata, T. Matsumiya, H. Namiki, M. Yoneyama, T. Fujita, PLoS ONE 7 (2012) e43031.
[31] M.A. Langereis, Q. Feng, F.J. van Kuppeveld, J. Virol. 87 (2013) 6314–6325.
[32] S. Najib, C. Martin-Romero, C. Gonzalez-Yanes, V. Sanchez-Margalet, Cell. Mol. Life Sci. 62 (2005) 36–43.
[33] J. Piotrowska, S.J. Hansen, N. Park, K. Jamka, P. Sarnow, K.E. Gustin, J. Virol. 84 (2010) 3654–3665.
[34] R.L. Finnen, K.R. Pangka, B.W. Banfield, J. Virol. 86 (2012) 8119–8130.
[35] I. Sola, C. Galan, P.A. Mateos-Gomez, L. Palacio, S. Zuniga, J.L. Cruz, F. Almazan, L. Enjuanes, J. Virol. 85 (2011) 5136–5149.
[36] K. Fujimura, F. Kano, M. Murata, RNA 14 (2008) 425–431.
[37] J.P. White, R.E. Lloyd, J. Virol. 85 (2011) 12442–12454.
[38] I.M. Cristea, J.W. Carroll, M.P. Rout, C.M. Rice, B.T. Chait, M.R. MacDonald, J. Biol. Chem. 281 (2006) 30269–30278.
[39] K.W. Dunn, M.M. Kamocka, J.H. McDonald, Am. J. Physiol. Cell Physiol. 300 (2011) C723–C742.
[40] A. David, B.P. Dolan, H.D. Hickman, J.J. Knowlton, G. Clavarino, P. Pierre, J.R. Bennink, J.W. Yewdell, J. Cell Biol. 197 (2012) 45–57.
[41] A. David, J.R. Bennink, J.W. Yewdell, Histochem. Cell Biol. 139 (2013) 501–504.
[42] F. Weber, V. Wagner, S.B. Rasmussen, R. Hartmann, S.R. Paludan, J. Virol. 80 (2006) 5059–5064.
[43] M.A. Restrepo-Hartwig, P. Ahlquist, J. Virol. 70 (1996) 8908–8916.
[44] R. Gorchakov, E. Frolova, I. Frolov, J. Virol. 79 (2005) 9397–9409.
[45] L. Breakwell, P. Dosenovic, G.B. Karlsson Hedestam, M. D'Amato, P. Liljestrom, J. Fazakerley, G.M. McInerney, J. Virol. 81 (2007) 8677–8684.
[46] H. Sadek, B. Hannack, E. Choe, J. Wang, S. Latif, M.G. Garry, D.J. Garry, J. Longgood, D.E. Frantz, E.N. Olson, J. Hsieh, J.W. Schneider, Proc. Natl. Acad. Sci. U.S.A. 105 (2008) 6063–6068.
[47] T.W. Han, M. Kato, S. Xie, L.C. Wu, H. Mirzaei, J. Pei, M. Chen, Y. Xie, J. Allen, G. Xiao, S.L. McKnight, Cell 149 (2012) 768–779.
[48] M. Kato, T.W. Han, S. Xie, K. Shi, X. Du, L.C. Wu, H. Mirzaei, E.J. Goldsmith, J. Longgood, J. Pei, N.V. Grishin, D.E. Frantz, J.W. Schneider, S. Chen, L. Li, M.R. Sawaya, D. Eisenberg, R. Tycko, S.L. McKnight, Cell 149 (2012) 753–767.
[49] B.W. Banfield, A.J. Mouland, C. McCormick, Viruses 6 (2014) 3500–3513.
[50] M.M. Emara, H. Liu, W.G. Davis, M.A. Brinton, J. Virol. 82 (2008) 10657–10670.